quantum reports

Tracked for Impact Factor

CITESCORE 3.3

Article

On the Holographic Spectral Effects of Time-Interval Subdivisions

Sky Nelson-Isaacs

Special Issue
100 Years of Quantum Mechanics

Edited by
Prof. Dr. Viktor Dodonov, Prof. Dr. Margarita A. Man'ko, Prof. Dr. Salomon S Mizrahi and Prof. Dr. Luis L. Sánchez-Soto

MDPI

https://doi.org/10.3390/quantum7010014

quantum reports

MDPI

Article

On the Holographic Spectral Effects of Time-Interval Subdivisions

Sky Nelson-Isaacs

Independent Researcher, El Cerrito, CA 94530, USA; theskyband@gmail.com

Abstract: Drawing on formal parallels between scalar diffraction theory and quantum mechanics, it is demonstrated that quantum wavefunction propagation requires a holographic model of time. Measurable time manifests between interactions as a duration which is encoded in the frequency domain. It is thus a unified entity, and attempts to subdivide these intervals introduce oscillatory artifacts or spectral broadening, altering the system's physical characteristics. Analogous to spatial holograms, where information is distributed across interference patterns, temporal intervals encode information as a discrete whole. This framework challenges the concept of continuous time evolution, suggesting instead that discrete trajectories define a frequency spectrum which holographically constructs the associated time interval, giving rise to the experimentally observed energy spread of particles in applications such as time-bin entanglement, ultra-fast light pulses, and the temporal double slit. A generalized model of quantum wavefunction propagation based on recursive Fourier transforms is discussed, and novel applications are proposed, including starlight analysis and quantum cryptography.

Keywords: quantum wavefunction propagation; scalar diffraction theory; spectral theory; quantum gravity; holographic spacetime intervals; non-locality; time–energy entanglement; quantum measurement; single-photon generation

1. Introduction

Due to the similar origins of Schrödinger's wave equation for wavefunction propagation and the propagation of light waves in scalar diffraction theory (SDT), it has long been understood that these two theories share a common formalism [1]. This common heritage allows one to treat time and space in a similar fashion, due to the existence of well-defined Fourier transforms and corresponding spectra for both spatial and temporal signals. Therefore, quantum wavefunction propagation can be formulated as a recursive Fourier transform (RFT) in both space and time, similar to the image formation process in scalar diffraction theory [2].

Having established a RFT process at the foundation of wavefunction propagation, it is immediately evident that propagation intervals cannot be subdivided without introducing distinctive changes in the frequency domain. This observation arises from the time–energy duality, where a temporal interval such as that corresponding to the propagation of an optical signal through a fiber is encoded as a spectrum in the frequency domain. Such a spectrum corresponds to an entire interval, and not any subdivision of the interval. In fact, it is readily shown that any attempt to define a smaller sub-interval introduces spectral artifacts which uniquely define the geometry of the perturbation. Spectrally, the whole is not the sum of the parts. This is a hallmark of holographic systems, whose spatial information is distributed across an entire region in the form of interference patterns, leading to non-local visual artifacts when broken into pieces.

check for updates

Academic Editor: Michael Kellman

Received: 29 January 2025
Revised: 24 February 2025
Accepted: 6 March 2025
Published: 19 March 2025

Citation: Nelson-Isaacs, S. On the Holographic Spectral Effects of Time-Interval Subdivisions. *Quantum Rep.* **2025**, *7*, 14. https://doi.org/10.3390/quantum7010014

Holographic time intervals have implications for both the foundations of quantum mechanics and interpreting experimental results, as well as suggesting new experimental setups. Holographic time intervals are "irreducible" or "indivisible" in the sense that if one makes a measurement at an intermediate time, one obtains a fundamentally different entity, such that the spectra of the partial segments that are generated do not sum to make up the original whole. In other words, there is a spectral difference between traveling from $A \rightarrow C$ on a path through B and actually traveling from $A \rightarrow B \rightarrow C$. Holographic time intervals encode information as a whole, such that intermediate measurements alter the spectral characteristics of the interval.

In the RFT model, the standard inclusion of time only as a continuous background parameter is modified. On one hand, unitary time evolution is trivially preserved, because the Fourier transform relies on a continuous time variable. However, this aspect of time evolution is inherently unmeasurable. Time in a measurable or experimental sense is limited to time intervals, whose finite boundaries appear as oscillations in the frequency domain. Such intervals of time are thus constructed by their frequency-domain components and have 'structure'. For instance, the structure of a time interval in a string of femtosecond laser pulses is the standing wave pattern of the photon pulses. They are not uniform, not arbitrarily shapeable, and not reducible to parts without changing their associated frequency components. These qualities manifest in the energy spectrum of statistical ensembles of particles in a given experimental setup, as is already demonstrated in numerous experimental results, including ultra-fast laser pulses [3,4] and temporal double-slit interference [5].

Because, similar to a hologram's spatial information, temporal information is distributed across a region of time, a notion of quantization is implied. Yet, time is not inherently quantized in the usual sense. Rather than thinking about time as a background parameter, time intervals emerge out of the trajectories of particles between interactions. The trajectory of a particle between interactions is inherently discrete, because the wavefunction propagation is due to the application of RFT, which is inherently a discrete process, similar to SDT. It is in this sense that measurable time intervals emerge discretely out of measurement interactions, and are thus discrete.

Holographic time refers to the concept that measurable time intervals are encoded as unified entities in the frequency domain, similar to how holograms store spatial information. Just as a hologram encodes the entire spatial structure of an object within an interference pattern, a holographic time interval stores its temporal characteristics as a whole, distributed across its spectral components. This encoding means that subdividing or measuring intermediate points within the interval alters the entire spectral pattern, demonstrating that the interval cannot be meaningfully reduced into independent parts. Consequently, the evolution of a system is determined by the global-phase structure of the interval rather than by continuous, local increments of time.

Time evolution has previously been studied in quantum mechanics in contexts similar to space evolution, namely diffractive effects [6], interference effects, and entanglement [7]. Applications include femtosecond laser pulses, high harmonic generation [8], single-photon generation [9], spontaneous parametric down conversion, photon arrival time, quantum computing and quantum sensing [10–12], and solitons [13].

In Section 2, a theoretical foundation is established for the remainder of the paper. In Section 3, the main argument is conveyed for the holographic nature of temporal intervals, and illustrated through an example of time-bin measurements. In Section 4, two novel predictions are made, and various well-known experimental setups are analyzed with respect to holographic temporal intervals. In Section 5, the new approach is compared to the standard quantum formalism, emphasizing their compatibility, and suggesting benefits provided by the new model. Appendices are provided which outline the relationship of

scalar diffraction theory and quantum wavefunction propagation, as well as the formal mathematical basis used.

2. Background

2.1. Definitions and Notation

The following definitions and notational conventions are used throughout the paper.

- A time interval is *irreducible* if a subdivision of the interval introduces new frequency components, such that the whole is not the sum of the parts.
- The Fourier transform of the wavefunction $\Psi(t)$ in the frequency domain is denoted by $\tilde{\Psi}(\omega)$.
- The *sinc* function is defined as:

$$sinc(\omega) = \frac{\sin(\omega)}{\omega}.$$

- The convolution theorem states that two functions multiplied together in one domain can be rewritten as a convolution in the dual domain, e.g.,

$$\{\tilde{a} * \tilde{b}\}(\omega) = \mathcal{F}\{a(\tau)b(\tau)\}. \tag{1}$$

- This relationship can also be expressed through consecutive use of the inverse and forward Fourier transform:

$$\{\tilde{a} * \tilde{b}\}(\omega_f) = \underset{\tau\to\omega_f}{\mathcal{F}}\left\{\underset{\omega\to\tau}{\mathcal{F}^{-1}}\left\{\tilde{a}(\omega)\right\}\underset{\omega\to\tau}{\mathcal{F}^{-1}}\left\{\tilde{b}(\omega)\right\}\right\}. \tag{2}$$

- In the above equations:
  - The subscripts under the Fourier transform symbol $\mathcal{F}$ indicate the initial and final domains of the transform.
  - Symbols such as τ, ω, and $\bar{\omega}$ are continuous, unmeasurable dummy parameters of integration.
  - The measurable coordinate in the frequency spectrum is denoted by ω_f, and the measurable event duration is denoted by T.

2.2. Representing Time in the Frequency Domain

In this approach, there are two notions of time. The first is unitary time, which advances continuously, allowing us to calculate how a system will evolve into the future. However, unitary time is unmeasurable; it enters the theory as the parameter of integration in the Fourier transform (or equivalently in the Schrödinger equation or the Feynman path integral), and thus has no definite value. Put another way, because time does not exist as an explicit variable in the frequency domain, and the Fourier transform is unitary and preserves information, it (time) cannot evolve continuously. Yet, another way to see the impossibility of continuous time in this model is that the spectrum of an instantaneous signal is not well-defined.

Instead, what we can measure are discrete coordinates or durations, which are not variables but constant data points which can readily be represented in the frequency domain, where they encode the frequency of oscillation of the spectrum.

We can gain an intuition for the effect of subdividing a temporal interval by considering the impact of truncating a digital audio signal using a sharp cutoff in the frequency domain. This truncation introduces oscillatory artifacts, analogous to the phenomena of Gibbs ringing or spectral broadening, where an approximation of a function with a sharp

transition exhibits ringing artifacts due to the truncation of its Fourier series or discrete Fourier transform representation, respectively.

A similar effect appears in digital imaging. The two-dimensional Fourier spectrum of an image encodes the rapidity of contrast variations over space. When certain digital filters apply hard cutoffs in the frequency domain, they introduce oscillatory artifacts or ripples in the image, more generally known as spectral leakage.

Similarly, it is proposed that, in quantum wavefunction propagation, subdividing a temporal interval introduces oscillatory artifacts in the frequency domain, emphasizing the coherence of the original interval.

Frequency space (parameterized by ω) plays a central role in this perspective, in that the time evolution of a quantum system is governed by the phase structure of its frequencies, rather than by explicit time parameters.

2.3. The Interaction of Signals

The close parallels between the formulation of quantum mechanics and scalar diffraction theory are reviewed in Appendix B. This equivalence can be readily seen (in one spatial dimension) using the propagator formulation to translate a free-particle wavefunction. Defining the propagator,

$$\begin{aligned} \mathbb{K}(x', x) &= \langle x'|e^{i\hat{p}x}|x\rangle \\ &= \int dk\, \langle x'|e^{i\hat{p}x}|k\rangle\, \langle k|x\rangle\,, \end{aligned} \tag{3}$$

where $\hat{p}$ is the momentum operator, the updated wavefunction is

$$\begin{aligned} \Psi(x') = \langle x'|e^{i\hat{p}x}|\Psi\rangle &= \int dx\, \langle x'|e^{i\hat{p}x}|x\rangle\, \langle x|\Psi\rangle \\ &= \int dx \int dk\, \langle x'|e^{i\hat{p}x}|k\rangle\, \langle k|x\rangle\, \langle x|\Psi\rangle \\ &= \int dk\, e^{ikx'} e^{iS_k(k)} \int dx\, e^{-ikx} \Psi(x) \\ &= \mathcal{F}^{-1}\Big\{ e^{iS_k(k)} \mathcal{F}\Big\{ \Psi(x) \Big\} \Big\}, \end{aligned} \tag{4}$$

where $S_k(k)$ is a phase. It is evident that space translation via Fourier transform is the result of a phase factor being applied in k-space, which can also be written as convolution in the x domain, $h(x) * \Psi(x)$, where h is the impulse response of the 'system',

$$h(x) = \mathcal{F}^{-1}\{e^{iS(x)}\}$$

Equation (4) is referred to as a recursive Fourier transform (RFT).

Relatedly, in signal processing, the interaction of temporal signals in the physical domain is accomplished by multiplication in the frequency domain, as described by the convolution theorem. This relationship is expressed as

$$c(t) = b(t) * a(t) = \mathcal{F}^{-1}\{\tilde{b}(\omega)\tilde{a}(\omega)\}, \tag{5}$$

Any interaction that alters the temporal properties of a signal can be represented as multiplication in ω-space.

In an analogous manner, a filter represents a non-local interaction in ω-space, achieved by multiplying two signals in t-space,

$$\tilde{a}(\omega) = \mathcal{F}\{f(t)g(t)\}, \tag{6}$$

This relationship reflects the dual nature of convolution and multiplication: an operation in one domain has a complementary effect in the other. For example, $f(t)$ could represent a carrier signal, and $g(t)$ a modulation function applied to the signal. The resulting product in t-space (amplitude modulation) corresponds to a convolution of their spectra in ω-space.

Combining Equations (5) and (6), a general interaction involves simultaneous effects in both t- and ω-spaces, reflecting the symmetry of Fourier duality,

$$c(t) = \mathcal{F}^{-1}\{\tilde{b}(\omega)\mathcal{F}\{f(t)g(t)\}\}. \tag{7}$$

Shifts in one domain correspond to phase changes in the dual domain, encapsulating the interplay between time and frequency.

Using these relationships, we can evolve the initial spectrum $\tilde{\Psi}_0(\omega)$ to a new time $\tau = T$ using the time-dependent Schrodinger equation, written in the following form:

$$\tilde{\Psi}(\omega_f) = \frac{1}{i\hbar}\int_0^T d\tau V(\tau)\int_{-\infty}^{\infty} d\omega\, e^{i\omega_f\tau}e^{-i\omega\tau}\tilde{\Psi}_0(\omega), \tag{8}$$

where the initial state $\tilde{\Psi}_0(\omega)$ could be, for instance, a Gaussian.

3. Subdividing Temporal Intervals

We now derive the main result. Consider the evolution of the energy eigenstates of a particle under a small perturbing potential. Starting with Equation (8), we use the following method to evaluate the expression:

- Rearrange factors such that the summation symbol or integral sign is as far as possible to the right;
- Remove the limits of integration so the temporal integral becomes a Fourier transform;
- Insert a masking function, $rect(t)$ (here, rect(t) is the rectangular function, defined as 1 for $|t| < 0.5$ and 0 otherwise. Subtracting the fraction $1/2$ from its argument moves its left edge to the origin, for convenience), so the integral is exact even under the extension of limits.

The new expression is

$$\tilde{\Psi}(\omega_f) = \frac{1}{i\hbar}\int_{-\infty}^{\infty} d\omega\tilde{\Psi}(\omega)\int_{-\infty}^{\infty} d\tau e^{i\omega_f\tau}V(\tau)rect\left(\frac{\tau}{T}-\frac{1}{2}\right)e^{-i\omega\tau}. \tag{9}$$

Next, the Fourier transform can be evaluated exactly, using the convolution as in Equation (2),

$$\begin{aligned}\tilde{\Psi}(\omega_f) &= \frac{1}{i\hbar}\int_{-\infty}^{\infty} d\omega\tilde{\Psi}_0(\omega)\underset{\tau\to\omega'}{\mathcal{F}}\left\{\underset{\bar{\omega}\to\tau}{\mathcal{F}^{-1}}\left\{T\exp\left(i(\bar{\omega}-\omega)T/2\right)sinc((\bar{\omega}-\omega)T/2)\right\}\underset{\bar{\omega}\to\tau}{\mathcal{F}^{-1}}\left\{\tilde{V}(\bar{\omega})\right\}\right\}\Big|_{\omega'=\omega_f} \\ &= \frac{1}{2\pi i\hbar}\int_{-\infty}^{\infty} d\omega\tilde{\Psi}_0(\omega)\left(G_0(\omega'-\omega)*\tilde{V}(\omega')\right)\Big|_{\omega'=\omega_f},\end{aligned} \tag{10}$$

where

$$G_0(\omega) \equiv Te^{i\omega T/2}sinc(\omega T/2), \tag{11}$$

is the Fourier transform of the *rect* function, known as the transfer function.

Here, we started with a photon in the state $\tilde{\Psi}_0(\omega)$ parameterized by the initial frequency variable, ω. We then reverse engineered the integrand of the time integral of the TDSE into the frequency domain parameterized by $\bar{\omega}$, transformed it into a convolution

parameterized by ω' using the convolution theorem, evaluated that distribution at the measurable value $\omega' = \omega_f$, and finally integrated over the initial states (ω), which amounts to a convolution over that variable. This process is described in [14].

In Equation (10), the integral over ω is recognized as a convolution, so in the case that the potential is time independent and the initial state is a single-frequency ω_0, we obtain the result

$$\begin{aligned} \tilde{\Psi}(\omega_f) &\propto \delta(\omega_f - \omega_0) * G(\omega_f) \\ &\propto G(\omega_f - \omega_0), \end{aligned} \tag{12}$$

which tells us how each individual frequency component is spread.

We now divide the time integral in the equation into two unequal segments of 1/3 and 2/3 in duration, respectively. Due to the nature of the Fourier transform and Multiplier Operator Theory, evaluating the time integral over contiguous segments is not the same as a single unbroken interval.

$$\begin{aligned} \tilde{\Psi}(\omega_f) &= \frac{1}{i\hbar}\int_{-\infty}^{\infty} d\omega \tilde{\Psi}_0(\omega) \int_0^{T/3} d\tau e^{i\omega_f \tau} e^{-i\bar{\omega}\tau} V(\tau) \\ &\quad + \frac{1}{i\hbar}\int_{-\infty}^{\infty} d\omega \tilde{\Psi}_0(\omega) \int_{T/3}^{T} d\tau e^{i\omega_f \tau} e^{-i\bar{\omega}\tau} V(\tau) \\ &= \frac{1}{2\pi i\hbar}\int_{-\infty}^{\infty} d\omega \tilde{\Psi}_0(\omega) \left(G_3(\omega' - \omega) * \tilde{V}(\omega') \right) \Big|_{\omega'=\omega_f} \end{aligned} \tag{13}$$

where

$$G_3(\omega) = \frac{T}{3} e^{i\omega T/6} sinc(\omega T/6) + \frac{2T}{3} e^{i2\omega T/6} sinc(2\omega T/6). \tag{14}$$

Equation (14) should be compared to Equation (11). The oscillating integrands $G_0(\omega)$ and $G_3(\omega)$ are plotted in Figure 1.

The result of decomposing or 'reducing' the whole interval from 0 to T to two intervals of unequal duration is to introduce oscillations in the spectrum. This represents a measurable distinction in the spectrum associated with the path $A \to C$ (on a timeline where B is implicit but not written) compared to the path $A \to B \to C$, where B is a boundary of the integration. Interestingly, we have said nothing of the cause of the segmentation or the nature of physical measurement. All we have done is identified *potential* subsections of a region. Apparently, the very act of identifying or defining such a subdivision affects the spectrum of the particle.

These two cases (subdivided or not subdivided) can be distinguished from each other by their spectral fingerprint. Except for a special case noted below, one can determine whether (and when) any sort of disturbance has happened along the journey of duration T by checking if these extra oscillations exist in the spectrum of the detected photons.

The introduction of additional frequency components when subdividing a temporal interval can be understood through Multiplier Operator Theory, where the application of rectangular functions to define sub-intervals acts as *sinc* filters in the frequency domain, generating new frequency components. According to the Mikhlin Multiplier Theorem, such multipliers in the frequency domain can be minimized with the use of smooth windowing filters, but in any case the spectra of the subdivided intervals will be modified by the windowing [15].

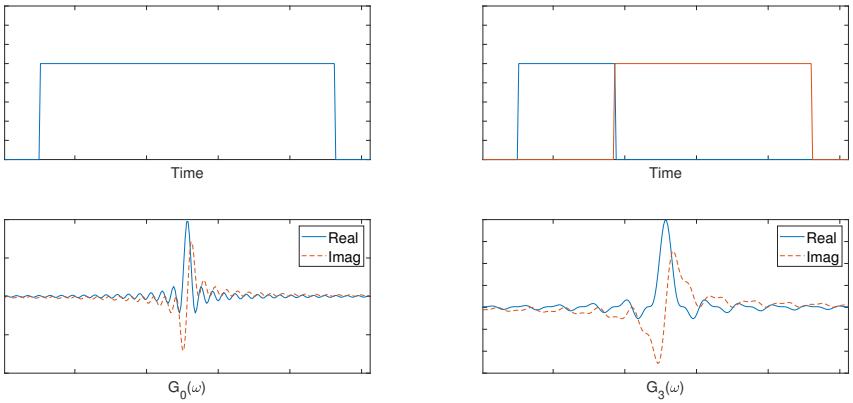

Figure 1. Spectrafor a single interval of duration T (**left**) compared to that for the same interval divided into 1/3 (blue) and 2/3 (orange) segments (**right**). The spectra are calculated using Equations (10) and (13).

Gaussian windows could be employed to experimentally minimize the spectral signatures of subdivision, to test whether these results are fundamental or methodology dependent.

Note that in the special case that one divides the temporal interval exactly in half, the spectrum is unaltered.

$$\begin{aligned}\tilde{\Psi}(\omega_f) &= \frac{1}{i\hbar}\int_{-\infty}^{\infty} d\omega \tilde{\Psi}_0(\omega)\int_0^{T/2} d\tau e^{i\omega_f\tau}e^{-i\omega\tau}V(\tau)\\ &\quad+\frac{1}{i\hbar}\int_{-\infty}^{\infty} d\omega \tilde{\Psi}_0(\omega)\int_{T/2}^{T} d\tau e^{i\omega_f\tau}e^{-i\omega\tau}V(\tau)\\ &= \frac{1}{i\hbar}\int_{-\infty}^{\infty} d\omega \tilde{\Psi}_0(\omega)\left(\left[e^{i\omega' T/4}+e^{i3\omega' T/4}\right]sinc(\omega' T/4)*\tilde{V}(\omega'-\omega)\right)\Big|_{\omega'=\omega_f}\\ &= \frac{1}{i\hbar}\int_{-\infty}^{\infty} d\omega \tilde{\Psi}_0(\omega)\left(Te^{i\omega T/2}sinc(\omega T/2)*\tilde{V}(\omega')\right)\Big|_{\omega'=\omega_f},\end{aligned} \tag{15}$$

where a trigonometric identity was used in the last step. This expression matches the result for the undivided interval in Equation (10). We can therefore subdivide an interval exactly in half and have no effect on the spectrum.

Demonstrating Holographic Time in a Time-Entangled State

To demonstrate this empirically, we can arrange to subdivide a time interval through the use of time bins. In the initial configuration, we create one sole time bin, of duration T. This represents a temporal interval of travel for a photon. In a secondary configuration we create two consecutive time bins of the same total duration. All the time bins are represented by rect functions in time. We can readily show that the latter condition generates extra spectral oscillations, distinguishing it from the initial configuration. The only difference between these two cases is our ability to distinguish between early arrival and late arrival within that window.

In a typical time–energy entanglement experiment, two identical photons (signal and idler) are generated from a single higher-energy photon through the process of spontaneous parametric down conversion (SPDC). The photons are correlated, in that they share a common joint spectral amplitude (JSA), $\phi(\omega_s, \omega_i)$.

Let's examine the frequency space wavefunction for the two distinct cases. The time bins will define the basis functions for our representation of the frequency space wavefunction. Using the standard process, we project the JSA onto the time bins in order to

determine the coefficients, c_k. Once those are known, the momentum space wavefunction is calculated as,

$$\tilde{\Psi}(\omega_s, \omega_i) = \sum_{k,m} \frac{c_{k,m}}{\sqrt{\Delta t_k \Delta t_m}} e^{i(\omega_s(t_k + \Delta t_k/2) + \omega_i(t_m + \Delta t_m/2))} \frac{\sin(\omega_s \Delta t_k/2)}{\omega_s/2} \frac{\sin(\omega_i \Delta t_m/2)}{\omega_i/2}.$$

In the initial configuration, with $k = m = 0$ we have a single bin of duration $\Delta t_0 = T$ which begins at $t_0 = 0$, so the expression above simplifies to,

$$\tilde{\Psi}(\omega_s, \omega_i) = c_{0,0} T e^{i(\omega_s + \omega_i)T/2} sinc(\omega_s T/2) sinc(\omega_i T/2). \tag{16}$$

Compare this with Equations (10) and (11) for the single-photon case.

The spectral distribution of the signal and idler photons is a simple sinusoid with a period of oscillation $2/T$, decaying away from the origin. This can be measured by counting the number of photons detected at each frequency.

In the second case, we define the early bin from $t = 0 \rightarrow T/3$ and the late bin from $t = T/3 \rightarrow T$, so that $\Delta t_0 = T/3$ and $\Delta t_1 = 2T/3$. Now, there are four combinations for either of the two photons to arrive in either of two time bins. The momentum space wavefunction becomes

$$\begin{aligned} \tilde{\Psi}(\omega_s, \omega_i) = {} & c_{0,0} \frac{T}{3} e^{-i(\omega_s + \omega_i)T/6} sinc(\omega_s T/6) sinc(\omega_i T/6) \\ & + c_{0,1} \frac{\sqrt{2}T}{3} e^{-i(\omega_s + 4\omega_i)T/6} sinc(\omega_s T/6) sinc(\omega_i T/3) \\ & + c_{1,0} \frac{\sqrt{2}T}{3} e^{-i(4\omega_s + \omega_i)T/6} sinc(\omega_s T/3) sinc(\omega_i T/6) \\ & + c_{1,1} \frac{2T}{3} e^{-i4(\omega_s + \omega_i)T/6} sinc(\omega_s T/3) sinc(\omega_i T/3) \end{aligned} \tag{17}$$

where factors of the form $\sqrt{\Delta t_k}$ are included to normalize each *sinc* function.

Equation (17) is the extension of Equation (10) to the case of two entangled particles. Comparing Equations (16) and (17), we see that the consequence of dividing the interval into parts is to remove the fundamental oscillation at $T/2$ and introduce harmonics at $T/6$ and $2T/6$ in the spectral domain.

By expressing quantum wavefunction propagation in terms of the Fourier transform, we leverage our understanding of dual spaces, namely that the spectrum changes when the domain of integration changes. Because the physical principles of quantum wavefunction propagation can be derived from the physics of these dual spaces, subdividing the integration domain has a physical effect, and thus the time bin intervals should be considered irreducible or holographic.

4. Holographic Time Intervals in Experiment

The usage of RFT for wavefunction propagation is consistent with existing experimental results. For instance, time-dependent potentials lead to the application of the Schrödinger equation to second order using the RFT methodology. However, we begin with two novel predictions based upon time-independent scenarios predicted by the holographic time interval hypothesis.

4.1. Novel Results

4.1.1. Measuring Stellar Distances Using Spectral Oscillations

A novel method is proposed for determining the distance of astronomical objects by identifying specific spectral oscillations introduced by the finite duration of light propaga-

tion. Unlike standard redshift and parallax techniques, this method exploits the holographic nature of temporal intervals according to Equation (10).

When photons travel from a distant star to Earth, the finite propagation time acts as a temporal boundary condition, modifying the frequency spectrum of the arriving photons. According to the holographic time hypothesis, this boundary condition encodes itself in the spectral domain as oscillatory sidebands spaced at intervals inversely proportional to the travel time.

For a given incoming frequency (e.g., one of the spectral lines of hydrogen), we write the initial state as $\tilde{\Psi}(\omega) = \delta(\omega - \omega_0)$, and the Fourier transformed potential in the time-independent case is $\tilde{V}(\omega) = \delta(\omega)$, resulting in Equation (12). The *sinc* function has maxima spaced at $\pm\pi$, or

$$\Delta f = \frac{1}{T}$$

where T is the travel time, so the principal spectral sidebands should be found at

$$f_1 = f_0 \pm \frac{1}{T}.$$

For Proxima Centauri, our nearest stellar neighbor at approximately 4.24 light years (1.34×10^8 s), the predicted spectral-oscillation spacing is approximately

$$\Delta f \approx 7.5 \times 10^{-9}\,\text{Hz},$$

a very small variation. To detect this, a frequency comb can be employed. The maximum fractional variation will occur if we minimize the carrier frequency. A good candidate in the hydrogen spectrum is the 21 cm radio frequency line (1.4×10^9 Hz). Current technology can resolve frequency differences on the order of 10^{-18} Hz (fractional resolution) [16], leading to an overall resolution at the given carrier frequency of

$$\sim 10^{-18} \times 10^9\,\text{Hz} = 10^{-9}\,\text{Hz},$$

so our current technology is capable of measuring the predicted spectral lobes. Assuming advances in technology in the near future, this method has the potential to be used over greater distances.

The measurement procedure is outlined as follows. Begin by capturing high-resolution spectra using an ultra-stable spectrograph equipped with an optical frequency comb which spans the carrier frequency of the starlight. The predicted side bands will generate a beat frequency with the frequency comb, on the order of nanohertz, which can be measured with standard electronics. The travel time between the star and the telescope can then be calculated using the inverse of the sideband spacing.

The procedure can be calibrated using laboratory light sources, which will display a broader spacing of the spectrum due to the very short laboratory optical travel time. Once starlight data are obtained, these can be compared with stars of known distances obtained through parallax to establish empirical correlations. For instance, Procyon's starlight travels 11.5 years to reach Earth, corresponding to a primary sideband spacing of $\Delta f \approx 2.8 \times 10^{-9}$ Hz. Corrections will need to be made for potential confounding factors such as interstellar medium dispersion and gravitational redshift.

Successful detection of spectral sidebands would provide direct empirical evidence supporting the concept of holographic time intervals, and could enable precise distance measurements of distant astronomical objects without reliance on standard candles or parallax. If dramatic increases in resolution capabilities are made, this procedure could potentially extend distance measurements to galaxies and quasars and provide a means to

verify the distance results obtained through the Doppler shift method, as well as provide an independent method for verifying Hubble's law.

4.1.2. Quantum Eavesdropping

In this theory, the entire spacetime path contributes to the observed spectrum, meaning the spectral artifacts reflect the shape of the whole trajectory in space and time. This includes any perturbations along its history, which would leave a distinctive spectral trace unique to the time at which the perturbation happened. Analyzing the spectrum could allow one to detect tampering by a third party (Eve) of a quantum signal (between Alice and Bob).

This fundamentally differs from the traditional approach by emphasizing the role of spacetime geometry in preserving and altering information, offering a direct way to detect eavesdroppers in a quantum channel. For instance, the spectrum in Equation (10) corresponds to a perturbation of the signal by an external system at a particular time $T/3$ along its path. The new method does not apply to individual photons whose quantum properties are disrupted due to the uncertainty principle, as is commonly done in discrete variable quantum computing; rather, the detection of eavesdropping depends upon the continuous spectrum of a collection of photons, similar to continuous variable quantum computing systems.

Experimental validation for this effect is significantly more feasible than for the astronomical case, as the much shorter path lengths involved in quantum optical setups result in substantially greater spectral spreads. Detecting spectral artifacts from intermediate interactions should be well within the capabilities of existing high-resolution spectroscopy and quantum optics instrumentation.

To illustrate a possible setup, a laser with a common telecom wavelength can be used, say 1550 nm. The light is channeled into a spool of single-mode optical fiber, approximately ten kilometers long, to simulate realistic transmission conditions in the lab. Before entering the fiber, the light is sampled and sent to an optical spectrum analyzer (OSA) to record its baseline spectrum, which should display a sharp, narrow peak centered at the laser's central frequency with minimal noise or sidebands. After passing through the fiber, the output light is sent to a second OSA to record the spectrum again for comparison.

To investigate how disturbances affect the spectral signature, controlled interference can be introduced at a midpoint along the fiber, such as gentle bends, pressure points, or the insertion of a weak optical coupler to simulate eavesdropping. The expectation is that these disturbances will alter the overall frequency content of the light according to Equation (10), producing small but measurable deviations in the spectrum.

By comparing the "before" and "after" spectra, the experiment aims to identify whether the holistic spacetime behavior of the continuous light stream creates a stable spectral fingerprint that reveals disturbances. The predicted results of this experiment could be explained through traditional ideas of resonance, where the frequency spectrum pattern is a standing wave due to back and forth reflections along the length of the channel. However, in the previous case when measuring starlight, it is clear that such a resonance model is not valid, since the light travels for interstellar distances and is not reflecting off the endpoints. Even without the classical resonant models of waves reflecting and interfering in a cavity, one still finds patterns of interference and spectral shifts due to the geometry of the path as a whole.

However, a key experimental challenge will be distinguishing genuine spectral artifacts from noise due to fiber imperfections. Random defects in an optical fiber waveguide can lead to intrinsic or extrinsic perturbations (e.g., optical fiber defects or microscopic bends, which collectively alter the refractive index profile and manifest as spectral artifacts) [17].

4.2. Confirmation of Existing Experimental Results

4.2.1. Temporal Modulation of Ultra-Fast Laser Pulses

In recent decades, the creation of chains of very short light pulses has become possible through high harmonic generation in the frequency domain [3]. Attosecond light pulses provide a very short-scale application of time's holographic nature.

It is interesting to think of a train of discrete attosecond pulses instead as a single entity with a temporal structure defined in the frequency domain. In our usual conception, a series of events are considered distinct and causal, i.e., the past pulses can affect the future pulses, but not the reverse. But, in this case, a series of pulses of extremely short duration in the time domain are generated from a comb in the frequency domain. The temporal characteristics are encoded as a whole within the phase structure of the frequency spectrum, set up more like a standing wave than a series of individual events. One can stretch the definition of the present moment to include a series of events, separated in time and yet occurring, in some sense, during the same moment.

In the process of high-harmonic generation (HHG), multiple harmonics are combined to produce ultra-short pulses. The exact pulse shape is determined by Fourier synthesis and is not a freely adjustable time-localized event, due to the structural constraints imposed by the time–frequency duality. The pulse chain is constructed as a whole, so, in a sense, the individual pulses are not separate objects. This is what is meant by holographic time.

One could ask why new methods are necessary given that the current methods adequately describe ultra-fast laser pulses. However, current methods do not allow for precise mapping of the temporal shape of the pulse. They rely on electron streaking and phase retrieval interferometry to infer the shape of the temporal envelope rather than directly measure it. Additionally, we do not have precise control over all aspects of amplitude and phase of the harmonics. Hence, the ability to craft precise shapes in the time domain and to confirm their accuracy is limited.

Attosecond pulses provide a nice illustration of the holographic structure of time intervals because their short duration maximizes the spectral broadening predicted by the theory. One uses the theory essentially in reverse to generate a laser pulse whose properties extend over a finite duration of time from the necessary spectral components which correlate to the desired shape of the pulse.

In this approach, time intervals are not defined as continuously adjustable parameters that can be arbitrarily shaped with continuous precision, but must be shaped as an entire interval via the harmonic spectrum.

4.2.2. Temporal Double Slit

The theory distinguishes between a single contiguous spacetime interval and subdivided intervals. In the temporal domain, this can be tested by splitting a photon's temporal path into two discrete segments. Following Lindner, et al. [5], two high-probability ionization windows are created within a single laser pulse by subjecting argon gas to femtosecond laser fields. Ionization of the argon atoms is allowed to occur within precisely two short time windows, separated by a brief duration where ionization is certain not to occur. The two time windows act as a double slit in time, producing fringes in the energy spectrum of the ejected electrons.

One can potentially modify the experiment by introducing a controlled disturbance to the photons prior to ionization (e.g., a weak laser pulse), which is predicted to have the effect of localizing the photons at a point partway along their path before ejecting the electrons. The distribution of kinetic energies for ejected electrons will exhibit the predicted spectral oscillations.

4.2.3. Bardeen Tunneling

A second-order prediction for electron tunneling through a voltage-biased junction can be made which builds upon Bardeen's first-order approximation. By expressing the TDSE in terms of RFT we capture higher-order effects [14]. A multi-lobed energy spectrum emerges, valid for short time intervals. The nested integrals of the TDSE are a clue to the non-instantaneous nature of second-order tunneling processes. Physically, this implies that electrons traversing the barrier exhibit transient energy fluctuations influenced by intermediate virtual states before reaching the final energy level. The RFT method expresses the resulting spectrum in terms of layered subspectra. This is, again, a hallmark of holographic systems which are constructed through gradual, non-local refinement, rather than point by point. By analyzing the spectral lobes, experimental techniques such as scanning tunneling microscopy (STM) and time-resolved photoemission spectroscopy could provide direct evidence of second-order tunneling dynamics, validating the predictive power of this approach and extending the applicability of Bardeen's theory to more complex quantum systems. Further second-order effects for four-wave mixing and optical experiments using the joint spectral amplitude are discussed in [14].

4.2.4. HOM Effect

In the HOM effect, two indistinguishable photons are arranged to interfere such that, when the arrival time of the photons match, both photons exit the interferometer through the same output port, reducing the coincidence detection rate between the output ports. The coherence is measured in the so-called "HOM dip", which depends on simultaneous arrival times of the photons with matching spectral characteristics.

Because of the dependency on arrival time, the HOM effect could be a useful way to confirm the relationship between the spectrum of a photon and the temporal subdivisions along its path. Since the temporal characteristics of the photons are encoded in their spectral phases, these phases can be measured by tracking the photon arrival time through the HOM dip [18].

Introducing spectral artifacts by subdividing the path of the incoming photons would result in variations of the time of arrival of the photons. The timing could be precisely correlated to the HOM dip in coincidence counts. Quantum-computing logic gates typically use the HOM dip as criteria turn on and off, so precise control of the arrival time of photons is crucial [10]. This theory predicts that the spectral envelope of a photon can be shaped through deliberate perturbations along its duration of flight.

4.2.5. Testing the Relationship Between Time and Frequency Domains

In this theory, the relationship between time and frequency domains is leveraged as a foundation for quantum dynamics. For instance, changes to the spectrum of laser light in an appropriate medium can generate a chain of laser pulses (mode-locked lasers) or an organized series of higher-frequency modes (high harmonic generation). Given that a finite spectrum corresponds to a non-instantaneous temporal interval, how do such changes in the spectrum translate to changes in the temporal domain? Is this relationship causal, in the sense that the beginning of the interval happens first? Is the temporal form a direct and instantaneous manifestation of the spectral changes? Do laser-pulse chains arise or disintegrate as a group or individually?

The emergence of standing wave patterns in a medium is generally thought of as a causal process, arising from the interference between waves emitted over a span of time and reflecting off the boundaries of the medium. Using the theory presented here, one could more carefully investigate the detailed process of formation or disintegration of a chain of pulses, or the lasing process within a laser when it is first turned on or turned off.

5. Discussion

5.1. The Role of Phase

An important aim of this analysis is to highlight the importance of the frequency domain spectrum—and particularly phase information—in temporal translation for both quantum wavefunction propagation (QWP) and scalar diffraction theory (SDT). While phase information is often ignored in signal processing (e.g., due to the limitations of photographic film or the focus on spectral magnitude), it plays a critical role in interference effects and system dynamics.

In Fourier analysis, phase information in k-space encodes spatial information in x-space. This insight motivates a $3+1$D formulation of quantum wavefunction propagation, where the same properties apply to space and to time. For example, an auditory tone can be shifted in time by t_0 via the transformation $\tilde{f}(\omega) \rightarrow \exp(i\omega t_0)\tilde{f}(\omega)$, and similarly, a spatial feature in a digital image can be shifted by Δx via $f(k) \rightarrow \exp(-ik\Delta x)f(k)$.

Modeling quantum dynamics after scalar diffraction theory provides a framework for symmetry between space and time, where the phase structure governs evolution. This approach reinforces the view of spacetime as fundamentally spectral, with phase information central to understanding quantum interactions and coherence.

5.2. Quantum Evolution in $3+1$ *Dimensions*

It is common in formulations of dynamics to treat dynamical variables such as displacement, velocity, or acceleration as dependent variables, parameterized by an unconstrained time parameter. Yet, even in the non-relativistic quantum formalism, a more sophisticated notion of time exists, namely in the distinction between parameters and coordinate intervals. Parameters, such as x and k, or t and ω, are unmeasurable dummy variables used in Fourier integrations to convert between dual domains. In contrast, coordinates $x_{(i)}$ and $t_{(i)}$ represent measurable intervals in space and time, while $k_{(i)}$ and $\omega_{(i)}$ correspond to distinct jumps in momentum states or energy levels. This distinction clarifies the static yet dynamically encoded nature of 3 + 1 D distributions in k^{μ}-space proposed here.

For example, a Fourier transform integrates out explicit time dependency, leaving a static ω distribution that cannot evolve in time but encodes dynamical information through its phase structure. This is analogous to a hologram, where 2D interference patterns encode 3D coordinates. Because the frequency domain does not contain a continuous-time variable, and the Fourier transform is unitary so it preserves information; in the RFT framework, continuous time cannot exist in either domain. Motion is represented as discrete updates in coordinate intervals during interactions, rather than continuous evolution, highlighting the encoded dynamical constraints within frequency space.

It was shown in Section 2.3 that the propagator can be represented as a discrete forward and inverse Fourier transform. Therefore, any propagation is carried out over finite, rather than infinitesimal distances and durations. Points in time or space in between the starting point and ending point of integration of the propagator are not individually defined. Distinguishing between parameters (of integration) which vary smoothly over the interval and the coordinates at the endpoints of the interval is a natural consequence of this approach. The latter are measurable and distinctly defined, whereas the former are not. This distinction is part of the standard theory of quantum mechanics, and emphasized in the RFT theory.

If we accept that the geometry of spacetime intervals and their spectra can be used to track dynamical interactions, and that expressions of the form Equation (4) (a propagator) can be applied to interactions in both space and time, we must conclude that intervals of space and time are discrete and holographic. The resulting description is symmetric

in these variables, providing a possible connection between the quantum formalism and special relativity.

5.3. Comparison to the Standard Quantum-Mechanics Formalism

The approach presented here distinguishes between unitary time, as an unmeasurable continuous parameter used in theoretical formulations, and discrete time, as a measurable interaction-defined coordinate interval. Unitary time exists only as an abstract, unmeasurable parameter, while measurable time consists of discrete intervals determined by interactions. The word 'time' itself will be typically reserved for the latter measurable interactions. Instead of treating time as a continuously evolving background parameter, this model views it as an emergent feature of discrete interactions. This aligns with some aspects of relational quantum mechanics, quantum gravity, and event-based models, but challenges standard interpretations of the Schrödinger equation and quantum field theory.

5.3.1. Relationship to the Time-Evolution Postulate (the Schrödinger Equation)

In standard quantum mechanics, time evolution is governed by the Schrödinger equation, which assumes a continuous-time parameter.

Standard QM Postulate 1. *The change in the state of a closed quantum system from t_0 to t_1 is described by the Schrödinger equation, i.e., the unitary transformation:*

$$|\psi_{t_1}\rangle = \hat{U}\,|\psi_{t_0}\rangle$$

The form of the unitary operator $\hat{U}$ follows directly from the Schrödinger equation, and depends only on the underlying Hamiltonian and the times t_0 and t_1.

In the model presented here, the same time parameter exists and the Schrödinger equation is unmodified, but it does not represent physical reality directly. Only discrete interaction-based time intervals are physically meaningful and measurable.

It was shown in [2], and summarized in Appendix C, that two new postulates (i.e., a 3 + 1 dimensional wave distribution governed by RFT evolution) can reproduce the Feynman path-integral formulation and the Schrödinger equation. Specifically, in the Schrödinger equation one integrates between two distinct measurable times, thereby defining a definite interval. In the (more general) RFT process, the time integration is treated as an indefinite integral (the transform) using a continuous dummy variable, while the limits of integration become values inside the integrand. Thus, there is both a calculational and an interpretational difference which does not invalidate, but can make more precise, the predictions of standard quantum mechanics via the Schrödinger equation.

For instance, in [14], a method for obtaining second-order corrections to the TDSE was presented using the RFT approach. Furthermore, the prediction made here of spectral signatures to starlight based on duration of travel is a unique prediction of this theory, showing where the paraxial approximation of the Schrödinger equation falls short.

To be clear, unitary time evolution is preserved in this model, since the Fourier transform uses a continuous-time parameter to transform between configuration space and the frequency domain. The Schrödinger equation, Heisenberg picture, and path-integral formulation all rely on unitary time evolution as a mathematical tool, and this is not altered in the present approach. Therefore, experimental setups that use precise continuous control parameters (e.g., ultra-fast laser experiments, Bose–Einstein condensates, or quantum tunneling experiments) still function exactly as expected. Such experiments do not directly measure a continuously evolving time; instead, they measure discrete interaction events (such as photon arrivals, transitions between quantum states, or interference patterns). Continuous evolution, while a useful concept, is 'hidden' from the experimenter.

For instance, in ultra-fast laser dynamics, pulse shaping and evolution are described by a continuous-time parameter, but photon detection times (from which we infer the pulse shape and spectrum) are discrete [19]. Similarly, the trajectory of a tunneling particle is discrete, but unitary calculations leading to the tunneling probability remain unchanged [20].

In Bose–Einstein condensates, condensate fraction measurements, phase coherence, or quantum state transitions are observed discretely, while the probabilities of each result are described through continuous-time evolution via the Gross–Pitaevskii equation [21].

In short, there is a measurable spectral signature associated with this model, in some cases validating previous predictions and in other cases generating new ones. Because trajectories are based upon spectral representations of temporal intervals, the frequency statistics of particles exiting a quantum device will have components dispersed above and below the central frequency in a predictable pattern dependent on the duration of the path.

In this model, it is not correct to think of time as an external parameter, nor as a background field that is quantized. Rather, trajectories themselves are quantized (as is evident from their description as RFT) and discrete time intervals emerge out of the description of specific trajectories.

5.3.2. Connection to the Measurement Postulate and the Born Rule

Holographic time intervals and the Fourier transform model of evolution are consistent with the standard measurement formalism. In quantum mechanics, it is already understood that there are two distinct notions of evolution, one unitary and the other discrete (Von Neumann's processes 2 and 1, respectively). The unclear relationship between these is the foundation of the quantum measurement problem or 'collapse of the wave function'.

Process 2 was described in the previous section (i.e., the Schrödinger equation). Process 1 was formalized by Dirac and Von Neumann [22], called the projection postulate:

Standard QM Postulate 2. *Consider a quantum system S whose pure states belong to a Hilbert space $\mathcal{H}$, and an observable A represented by a self-adjoint operator $\hat{A}$ on $\mathcal{H}$ which has a discrete spectrum. If A is measured when S is in a pure state $|\psi\rangle$ and the value α is found, then, after the measurement, S is in the pure state $\Pi_\alpha|\psi\rangle$, where Π_α is the operator on $\mathcal{H}$ of orthogonal projection onto the subspace of eigenstates of $\hat{A}$ with eigenvalue α.*

The result is a discrete transition from the previously measured state which has been spread into an array of eigenstates of a measurement operator, then evolved unitarily in time (though 'hidden'), before being truncated to a single state, resulting in a finite time interval.

Sudbery explains, "From the earliest adumbrations of quantum theory by Bohr and Heisenberg, it was recognised that a central feature of the theory was that observation had an inescapable effect on a physical system; after Schrödinger's formulation of the theory in terms of wavefunctions, this came to be known as the 'collapse of the wave function' " [22].

The model presented here perhaps more clearly delineates these two concepts, as they appear naturally in a single theory as continuous parameters (non-measurable unitary Fourier integration dummy variables) and discrete coordinates (measurable values which appear as frequencies in the dual domain). The introduction of probabilities with the Born rule already implies a non-continuous structure in practical observations.

Thus, the approach presented here is consistent with the traditional model of Von Neumann evolution and its probabilistic interpretation, and in fact may provide an explanation for the source of these principles; namely, Fourier space duality, which is central to both approaches.

5.3.3. The Born Rule

The relationship between the 3 + 1 dimensional distribution made possible by the RFT model (see Section 5.2) and the probabilistic interpretation of the standard quantum mechanical wavefunction (i.e., the Born rule) is briefly examined in [2] in relationship to the Parseval–Plancheral theorem. Through this theorem, the squared norm of the distribution in the time domain is equal to the squared norm of the dual distribution in the frequency domain (because the Fourier transform is unitary), reinforcing that either distribution may be interpreted as a normalizable probability distribution.

Horwitz examines this relationship in the context of quantum gravity, discussed briefly in Section 5.4 [23]. The author shows that the probabilistic interpretation of the wavefunction (i.e., the Born rule) emerges naturally from the Fourier transform's role in preserving norms between position and momentum spaces.

5.3.4. A Multi-Block Universe

From special relativity, one has the model of a block universe in which spacetime trajectories are laid out as a whole, and time evolution is seen as the unfolding of a predetermined trajectory through spacetime. A multi-block universe extends this concept to accommodate branching of the wavefunction due to measurement interactions, a concept resulting from the superposition principle of quantum mechanics.

In a multi-block universe, segments of evolution are defined by a single-block universe description, consistent with special relativity. However, such evolution is punctuated by the splitting of 3 + 1 dimensional spacetime trajectories into mutually exclusive branches. This is the standard measurement problem in the context of a multi-block universe, and is naturally resolved into a single measurement result in the usual way using one's preferred collapse mechanism in quantum mechanics.

A multi-block universe is essential to the model proposed here, as it allows multiple trajectories defined in the frequency domain to evolve simultaneously while also accommodating free choices by an outside experimenter. The difference between a whole trajectory (e.g., from Sun to Earth) and a broken trajectory (e.g., from Sun to satellite to Earth) is described by distinct frequency domain phase distributions within distinct blocks.

In this model, the multi-block universe concept extends the standard block universe by allowing distinct frequency-domain trajectories to evolve simultaneously. Each 'block' represents a discrete time interval encoded as a holographic whole, with subdivisions corresponding to separate frequency patterns. Measurement interactions cause branching, where each branch maintains its own spectral signature. This approach aligns with the non-local and discrete nature of holographic time intervals, while preserving the deterministic structure of spacetime within each block. Consequently, the model offers a potential framework for integrating quantum measurements with relativistic spacetime, without relying on continuous time evolution.

5.4. Consistency with General Relativity and Theories of Quantum Gravity

The notion of holographic time intervals presented here shows promising compatibility with the theory of general relativity, which rejects the notion of a global clock. In general relativity, measurements of time intervals are relative to the observer, and are therefore defined by interactions, similar to the proposal put forward here. A number of existing theories of quantum gravity will be briefly compared to the current proposal.

As discussed in Section 5.3.3, Horwitz ensures covariance in curved spacetime by redefining the Fourier transform, the scalar product, and momentum operator to include the metric tensor $g_{\mu\nu}(x)$ and applying these to the Parseval–Plancherel theorem [23]. By incorporating the measure $\sqrt{g(x)}\, d^4x$ and modifying the momentum operator to remain

self-adjoint, the quantum probability interpretation via the Born rule becomes consistent with local diffeomorphisms. It is therefore promising that the theory presented here, grounded in similar mathematics, may be a candidate for a theory of quantum gravity.

In causal set theory (CST), time emerges as the causal ordering of events, and again global time is rejected. In the theory put forward here, reducing a single time interval to a sequence of multiple shorter segments implies a causal relationship between the segments. Instead of a continuous background parameter, the coordinates of successive interactions (which show up as frequencies in the dual space) stitch together the segments in a causal chain, marking the end of one segment and the beginning of the next.

In AdS/CFT holography, gravitational effects and spacetime itself are encoded into the boundary of anti-deSitter space, emerging as particle interactions in a conformal field theory in fewer dimensions. Some parallels might be drawn to the implicit encoding of spacetime trajectories in the frequency domain, as prescribed here.

It should be recalled also that in an actual holographic picture, the coordinates of features in space correspond to frequencies in the holographic interference pattern. Thus, the theory on which holographic spacetime intervals is based is fundamentally holographic, maybe more so than AdS/CFT, which simply borrows the notion of 'encoding on the boundary' as an analog, not a direct description.

In the theory of loop quantum gravity, geometrical entities like area and volume are associated with operators that define spectra, with some potential similarity to the new theory in which the temporal interval of a trajectory corresponds to a unique spectrum, leading to the notion of discrete holographic intervals.

In summary, holographic time intervals resulting from the RFT propagation methodology provide a model of time which is discrete and interaction-based. It should be explored whether spectrum-based time intervals are compatible with relativistic invariance.

6. Conclusions

In this study, it was shown that time intervals are encoded as a whole in the spectral fingerprint of a particle, e.g., photon. Emphasizing the similarity between quantum wavefunction propagation and scalar diffraction theory, it was shown that any subdivision or intermediate measurement along a temporal interval will result in spectral artifacts, making it evident that the whole interval and the partial interval are fundamentally different, and that they are to be considered as distinct, discrete wavefunction branches. As a corollary, it is predicted that photons of cosmic origin should retain a spectral fingerprint encoding their duration of travel, potentially providing a novel method for measuring astronomical distances.

Funding: This research received no external funding.

Institutional Review Board Statement: Not applicable.

Informed Consent Statement: Not applicable.

Data Availability Statement: The original contributions presented in this study are included in the article. Further inquiries can be directed to the corresponding author.

Conflicts of Interest: The authors declare no conflict of interest.

Appendix A. Overview of Quantum Wavefunction Dynamics in RFT Model

Time intervals should be treated differently depending on whether the Hamiltonian is time-independent or time-dependent. This can be seen through an analogy between spatial propagation and temporal evolution. In scalar diffraction theory, the propagation of an

optical wavefront across space is accomplished through the application of a phase factor in the frequency domain. A single Fourier transform converts the incoming two-dimensional wavefront into the frequency domain, whereupon a frequency-dependent phase factor is applied to appropriately update the phases of each frequency component, and then an inverse Fourier transform is applied, resulting in a spatially translated image.

It is possible to represent quantum wavefunction propagation in the same way for time-independent systems. In such cases, a single forward and reverse Fourier transform is required to propagate the wavefunction, with the appropriate phase factor applied in the frequency domain.

In the case of a time-dependent Hamiltonian, the Feynman path integral can be written as a recursion of forward and inverse Fourier transforms with appropriate phase factors, sliced at infinitesimal time intervals (see Appendix C) [2]. This is analogous to the spatial propagation of an optical wave in which a new aperture is encountered at every small step.

In the former case, the usage of RFT through a single time-evolution cycle corresponds to a novel holographic understanding of time intervals. This leads to novel predictions, such as modifications of the spectrum of starlight based upon duration of travel, or novel methods of detecting eavesdropping in quantum communication. This effect is not predicted by standard quantum mechanics, although it is simply an application of temporal diffraction.

In the latter case, infinitesimal time slices are necessary in order to invoke the Taylor series, and the result is useful for improving second-order calculations using the standard TDSE. In this case, the theory does not generate new predictions but provides a strong theoretical foundation for understanding existing experimental results.

Appendix A.1. Single-Step Fourier Transform for a Time-Independent Evolution

In scalar diffraction theory, the propagation of an optical wavefront from one plane to another is described by a single forward Fourier transform, multiplication by a phase factor representing free-space propagation, and an inverse Fourier transform to return to the spatial domain. This single-step process works because the entire spatial interval is treated as a boundary-value problem, with well-defined initial and final conditions. There is no need to break the propagation into incremental steps, as the Fourier transform inherently encodes the entire spatial structure of the wavefront. This is typically the situation with a single aperture in an optical imaging system.

Time evolution in quantum mechanics can be understood analogously. For a system governed by a time-independent Hamiltonian, the wavefunction evolves according to a single exponential phase factor, $e^{-iHt/\hbar}$, which represents the entire temporal interval as a unified entity. In this case, the time evolution is conceptually equivalent to a single forward and inverse Fourier transform, reflecting the fact that the entire interval is encoded in the frequency domain as a whole. This holographic view implies that, in the case of a time-independent Hamiltonian, measurable temporal intervals are irreducible, much like the spatial intervals in diffraction.

Appendix A.2. RFT for Time-Dependent Evolution

When the Hamiltonian is time-dependent or the system undergoes interactions at intermediate times, the analogy shifts from free-space propagation to the case of light passing through multiple spatial filters or apertures. In spatial optics, each filter or aperture modifies the wavefront, necessitating a forward Fourier transform to analyze the wavefront in the frequency domain, application of the filter's transfer function, and an inverse Fourier transform to return to the spatial domain. When multiple filters are present, this process must be repeated sequentially.

Similarly, in quantum mechanics, time-dependent evolution requires breaking the temporal interval into smaller segments. Each segment is treated as a short-duration evolution, where the RFT is applied to evolve the wavefunction incrementally. This iterative process accounts for changes in the Hamiltonian or external interactions at each step. Notably, this approach relies on the Taylor series expansion of the time evolution operator, which is valid only for small time intervals. Consequently, the recursive nature of the Fourier transforms is associated with second-order corrections, aligning with standard quantum mechanics' predictions for systems experiencing time-dependent perturbations.

Appendix A.3. Implications for Temporal Intervals and Experimental Predictions

The distinction between single-step and RFT has profound implications for interpreting temporal intervals. In the case of starlight, where photons travel over extremely long durations with no intermediate interactions, the temporal interval acts as a single holographic entity encoded in the frequency domain. This results in first-order spectral side lobes that cannot be explained by standard quantum mechanics, as there is no incremental evolution to produce second-order corrections.

Conversely, in tunneling experiments, where electrons traverse a potential barrier over very short durations, the RFT approach applies naturally. The Taylor series expansion is valid for these short intervals, and the second-order corrections predicted by this approach align with the established results of Bardeen's tunneling theory. Thus, the spectral side lobes observed in tunneling are not fundamentally new predictions but rather refinements of standard quantum mechanical effects.

Appendix B. Similarities Between Scalar Diffraction Theory and Quantum Wavefunction Propagation

Scalar diffraction theory (SDT) describes how an optical wavefront in two spatial dimensions changes as it propagates in a third spatial dimension. It utilizes both x-space and k-space to do so.

In SDT, an optical wavefront is propagated by multiplying its k-space representation by an amplitude transfer function. More generally, any filter can be applied to a signal by convolution in x-space or multiplication in k-space.

Similarly, in quantum mechanics (QM), the propagation of a wavefunction (or quantum wavefunction propagation, QWP) is encapsulated in the propagator, also defined in k-space. In both instances, propagation of a signal in spacetime involves multiplication by a phase factor in k-space.

The starting point for scalar diffraction theory is the Huygens–Fresnel equation, describing the propagation and consequent image formation due to an incoming wavefront affected by an aperture that propagates to a screen. If ξ and η correspond to the horizontal and vertical directions on the aperture of the imaging device, an integral is performed over the entire aperture for each point (x', y') on the viewing screen. Labeling the original waveform $U(\xi, \eta)$, the Huygens–Fresnel equation is [24]

$$\begin{aligned} U(x', y') &\propto \int d\xi d\eta U(\xi, \eta) \frac{\exp(ikr_{01})}{r_{01}^2} \\ &\propto \int d\xi d\eta U(\xi, \eta) \frac{\exp\left(ik\sqrt{z^2 + (x' - \xi)^2 + (y' - \eta)^2}\right)}{z^2 + (x' - \xi)^2 + (y' - \eta)^2}, \end{aligned} \tag{A1}$$

When combined with Fresnel's quadratic wavefront curvature approximation, the image on a screen under Fresnel diffraction is proportional to

$$\begin{aligned} U(x',y') &\approx \int d\xi d\eta U(\xi,\eta) \exp\left(\frac{ik}{2z}[(x'-\xi)^2+(y'-\eta)^2]\right) \\ &\approx \int d\xi d\eta U(\xi,\eta) e^{\frac{ik}{2z}(\xi^2+\eta^2)} e^{-i\frac{2\pi}{\lambda z}(x'\xi+y'\eta)} \\ &\approx \mathcal{F}^{-1}\left\{e^{\frac{ik}{2z}(\xi^2+\eta^2)}\mathcal{F}\{U(x,y)\}\right\}. \end{aligned} \tag{A2}$$

where a quadratic constant-phase factor of the form $\exp((x')^2+(y')^2)$ has been pulled out of the integral and omitted for the sake of clarity.

Note that when light passes through an aperture in $\vec{x}-$space, the spatial parameters ξ and η describing the aperture become scaled frequency parameters in k-space,

$$\begin{aligned} k_x &= \frac{2\pi\xi}{\lambda z} \\ k_y &= \frac{2\pi\eta}{\lambda z}, \end{aligned} \tag{A3}$$

where z is the distance to the screen, Equation (A2) can be written

$$\begin{aligned} U(x',y') &\propto \int\int d\xi d\eta\, \tilde{U}\left(\frac{2\pi\xi}{\lambda z},\frac{2\pi\eta}{\lambda z}\right) h\left(x'-\frac{2\pi\xi}{\lambda z},y'-\frac{2\pi\eta}{\lambda z}\right) \\ &\propto \tilde{U}(\xi,\eta) * h(\xi,\eta), \end{aligned} \tag{A4}$$

where $\tilde{U}$ is the Fourier transform of the incoming wavefront, and the convolution kernel $h(x,y)$ is called the impulse response, which is the inverse Fourier transform of the amplitude transfer function.

Appendix C. Formulating the Path Integral with RFT

Consider the following expression for a path integral,

$$\begin{aligned} \Psi(x_N,t_N) &= \int \mathcal{D}x\mathcal{D}k \exp\left(i\int_{t_i}^{t_f}(k\dot{x}-H)\,dt\right)\Psi(x_0,t_0) \\ &\approx \int\int \prod_{j=0}^{N-1} dx_j \frac{dk_j}{2\pi} \exp\left(i(k_j\frac{x_{j+1}-x_j}{\tau}-H)\tau\right)\Psi(x_0,t_0) \\ &= \prod_{j=0}^{N-1}\int \frac{dk_j}{2\pi}\exp(ik_jx_{j+1})\int dx_j \exp(-ik_jx_j)\exp(-iH\tau)\Psi(x_0,t_0) \\ \{N=2\} &\Rightarrow \mathcal{F}^{-1}_{k_1}\{e^{-i\frac{k_1^2}{2m}\tau}\mathcal{F}_{x_1}\{e^{iV(x_1)\tau}\mathcal{F}^{-1}_{k_0}\{e^{-i\frac{k_0^2}{2m}\tau}\mathcal{F}_{x_0}\{e^{iV(x_0)\tau}\Psi(x_0,t_0)\}\}\}\} \end{aligned} \tag{A5}$$

where k_j and x_j are free parameters of momentum and position inserted at the jth time step, and the Hamiltonian is $H=H(k_j,x_j)$. In the second line, we have passed from an integral to a Reimann sum, where $\tau=(t_f-t_i)/N$ is a small time interval. In the last line, we have passed to an explicit representation with $N=2$, and $\mathcal{F}_x$ refers, for instance, to a transform specifically over the x parameter.

As is well known, and evaluated in detail in [2], the Schrödinger equation can be derived from the Feynman path integral, and is also analogous to the paraxial approximation of scalar diffraction theory. Thus, the Schrödinger equation is not fundamentally modified by the reformulation via RFT.

Appendix C.1. Incorporating the Time Dimension into the RFT Method

The Feynman path integral in Equation (A5) expresses quantum evolution as an integral over all possible paths, where a spacetime path is defined as "a sequence of configurations for successive times" [25]. Through time slicing, one allows the spatial path to vary over all possible spatial trajectories, but always along a specific temporal trajectory. A single time slice can be rewritten using convolution with the free-particle propagator:

$$\Psi(x_1) = h_x * (e^{iV(x_1)\tau}\Psi(x_0)), \tag{A6}$$

where $h_x(x_j) \propto \exp\,(i\frac{x_j^2 m}{2\tau})$.

The time evolution of the wavefunction can also be represented via convolution in the time domain:

$$\Psi(t_{j+1}) = \delta(t_j - \tau) * \Psi(t_j) \tag{A7}$$

$$= \mathcal{F}_\omega^{-1}\{e^{i\omega_j\tau}\mathcal{F}_t\{\Psi(t_j)\}\}. \tag{A8}$$

This transformation leverages the shift property of the Fourier transform to express time evolution explicitly in the frequency domain.

A single time slice of the path integral can thus be rewritten as:

$$\Psi(x_{j+1}, t_{j+1}) \propto \left(\delta(t_j - \tau)\exp\,(i\frac{x_j^2 m}{2t_j})\right) * \left(e^{iV(x)\tau}\Psi(x_j, t_j)\right), \tag{A9}$$

where successive time slices apply this relationship recursively.

This reformulation suggests that instead of infinitesimal time slicing, explicit Fourier domain transformations provide an equivalent framework, emphasizing interactions rather than continuous time evolution.

References

1. Marte, M.A.M.; Stenholm, S. Paraxial light and atom optics: The optical Schrödinger equation and beyond. *Phys. Rev. A* **1997**, *56*, 2940–2953. [CrossRef]
2. Nelson-Isaacs, S.E. Spacetime Paths as a Whole. *Quantum Rep.* **2021**, *3*, 13–41. [CrossRef]
3. Tzallas, P.; Charalambidis, D.; Papadogiannis, N.A.; Witte, K.; Tsakiris, G.D. Direct observation of attosecond light bunching. *Nature* **2003**, *426*, 267–271. [CrossRef]
4. Agostini, P.; DiMauro, L.F. The physics of attosecond light pulses. *Rep. Prog. Phys.* **2004**, *67*, 813–855. [CrossRef]
5. Lindner, F.; Schätzel, M.G.; Walther, H.; Baltuška, A.; Goulielmakis, E.; Krausz, F.; Milošević, D.B.; Bauer, D.; Becker, W.; Paulus, G.G. Attosecond Double-Slit Experiment. *Phys. Rev. Lett.* **2005**, *95*, 040401. [CrossRef]
6. Moshinsky, M. Diffraction in Time. *Phys. Rev.* **1952**, *88*, 625–631. [CrossRef]
7. White, S.J.U.; Polino, E.; Ghafari, F.; Joch, D.J.; Villegas-Aguilar, L.; Shalm, L.K.; Verma, V.B.; Huber, M.; Tischler, N. A robust approach for time-bin encoded photonic quantum information protocols. *Npj Quantum Inf.* **2019**, *5*, 23. [CrossRef]
8. Tate, J.; Auguste, T.; Muller, H.G.; Salières, P.; Agostini, P.; DiMauro, L.F. Scaling of wave-packet dynamics in an intense midinfrared field. *Phys. Rev. Lett.* **2007**, *98*, 013901. [CrossRef]
9. Varga, J.J.M.; Lasa-Alonso, J.; Molezuelas-Ferreras, M.; Tischler, N.; Molina-Terriza, G. Bandwidth control of the biphoton wavefunction exploiting spatio-temporal correlations. *Optica* **2015**, *2*, 438–443. [CrossRef]
10. Ge, H.; Tomita, A.; Okamoto, A.; Ogawa, K. Reduction of the two-photon temporal distinguishability for measurement-device-independent quantum key distribution. *Opt. Lett.* **2024**, *49*, 822–825. [CrossRef]
11. Franson, J.D.; Jacobs, B.C.; Pittman, T.B. Quantum computing using single photons and the Zeno effect. *Phys. Rev. A* **2004**, *70*, 062302. [CrossRef]
12. Wahl, M.; Röhlicke, T.; Kulisch, S.; Rohilla, S.; Krämer, B.; Hocke, A.C. Photon arrival time tagging with many channels, sub-nanosecond deadtime, very high throughput, and fiber optic remote synchronization. *Rev. Sci. Instrum.* **2020**, *91*, 1. [CrossRef]

13. Brahms, C.; Travers, J.C. HISOL: High-energy soliton dynamics enable ultrafast far-ultraviolet laser sources. *APL Photonics* **2024**, *9*, 050901.
14. Nelson-Isaacs, S. Eliminating the Second-Order Time Dependence from the Time Dependent Schrödinger Equation Using Recursive Fourier Transforms. *Quantum Rep.* **2024**, *6*, 323–348. [CrossRef]
15. Mikhlin, S.G. *Multidimensional Singular Integrals and Integral Equations*; International Series of Monographs in Pure and Applied Mathematics; Armstrong, A.H., Translator; Pergamon Press: Oxford, UK, 1965; Volume 83.
16. Fortier, T.; Baumann, E. 20 years of developments in optical frequency comb technology and applications. *Commun. Phys.* **2019**, *2*, 153. [CrossRef]
17. Garito, A.F.; Wang, J.; Gao, R. Effects of Random Perturbations in Plastic Optical Fibers. *Science* **1998**, *281*, 962–967. [CrossRef] [PubMed]
18. Li, X.; Chen, J.; Voss, P.; Sharping, J.; Kumar, P. All-fiber photon-pair source for quantum communications: Improved generation of correlated photons. *Opt. Express* **2004**, *12*, 3737–3744. [CrossRef]
19. Kim, Y.; Vogel, S.S. Measuring two-photon microscopy ultrafast laser pulse duration at the sample plane using time-correlated single-photon counting. *J. Biomed. Opt.* **2020**, *25*, 014516. [CrossRef]
20. Ast, C.R.; Jäck, B.; Senkpiel, J.; Eltschka, M.; Etzkorn, M.; Ankerhold, J.; Kern, K. Sensing the quantum limit in scanning tunnelling spectroscopy. *Nat. Commun.* **2016**, *7*, 13009. [CrossRef]
21. Ketterle, W. Experimental Studies of Bose-Einstein Condensates. *Phys. Today* **1999**, *52*, 30–35. [CrossRef]
22. Sudbery, A. Whose projection postulate? *arXiv* **2024**, arXiv:2402.15280v2. Available online: https://arxiv.org/abs/2402.15280v2 (accessed on 11 November 2024).
23. Horwitz, L.P. Fourier Transform, Quantum Mechanics and Quantum Field Theory on the Manifold of General Relativity. *Eur. Phys. J. Plus* **2020**, *135*, 479.
24. Goodman, J.W. *Introduction to Fourier Optics*, 3rd ed.; McGraw-Hill Companies Inc.: New York, NY, USA, 2004; pp. 55–61.
25. Feynman, R.P. Space-Time Approach to Non-Relativistic Quantum Mechanics. *Rev. Mod. Phys.* **1948**, *20*, 367–387. [CrossRef]